M$^{\text{odeling}}$MC$^{\text{omputing}}$ $_{\text{athematical}}$

MHD flow of hybrid nanofluid past a stretching sheet: double stratification and multiple slips effects

Yahaya R. I.[1], Ali F. M.[1,2], Arifin N. M.[1,2], Khashi'ie N. S.[3], Isa S. S. P. M.[1,4]

[1]*Institute for Mathematical Research, Universiti Putra Malaysia,*
43400 Serdang, Selangor, Malaysia
[2]*Department of Mathematics, Universiti Putra Malaysia,*
43400 Serdang, Selangor, Malaysia
[3]*Fakulti Teknologi Kejuruteraan Mekanikal dan Pembuatan, Universiti Teknikal Malaysia Melaka,*
Hang Tuah Jaya, 76100 Durian Tunggal, Melaka, Malaysia
[4]*Centre of Foundation Studies For Agricultural Science, Universiti Putra Malaysia,*
43400 Serdang, Selangor, Malaysia

Studies of hybrid nanofluids flowing over various physical geometries and conditions are popular among researchers to understand the behavior of these fluids. Thenceforth, the numerical solutions for hybrid Ag-CuO/H_2O nanofluid flow over a stretching sheet with suction, magnetic field, double stratification, and multiple slips effects are analyzed in the present study. Governing equations and boundary conditions are introduced to describe the flow problem. Then, similarity variables are applied to transform the equations into non-linear ordinary differential equations and boundary conditions. The numerical computation for the problem is done in Matlab (bvp4c solver), and the results are presented in tables and graphs. It is found that the rise in solutal slip and stratification parameters reduces the Sherwood number. Meanwhile, the increase in thermal slip and stratification parameters lowers the Nusselt number. The skin friction coefficient is observed to increase with the augmentation of the hydrodynamic slip parameter.

1. Introduction

The suspension of two or more different nanoparticles with a size of less than $100\,\text{nm}$ in a base fluid produces a new generation of nanofluid, known as hybrid nanofluid [1]. The usual combination of nanoparticles is from carbon nanotubes, oxide nanoparticles, and metallic nanoparticles dispersed in a base fluid, usually water (H_2O), organic fluids, engine oils, and polymeric solutions. Hybrid nanofluids have similar applications to nanofluids in all fields of heat transfer, such as in biomedical, air-conditioning systems, heat exchangers, coolant in machining and manufacturing, solar energy, and transportation [1, 2]. However, the mixture of dissimilar nanoparticles with different characteristics makes hybrid nanofluids more superior to nanofluids and other conventional heat transfer fluids in terms of higher thermal conductivity and better thermophysical properties. Fluid flow over a stretching sheet is significant in various industrial and manufacturing processes. For example, fluid processing units operated on roller belts, paper industry and extrusion process, drawing of copper wires, manufacturing of aluminum bottle process, and production of rubber and plastic sheets [3, 4]. Devi and Devi [5] studied the flow of hybrid nanofluid over a stretching sheet with suction and magnetic field. In this study, Cu-Al$_2$O$_3$/H_2O hybrid nanofluid was found to have a higher heat transfer rate than the Cu/H_2O nanofluid. The greater efficiency of hybrid nanofluid compared to nanofluid was also agreed upon by Prakash and Devi [6] and Hayat and Nadeem [2] in studies involving different flow conditions
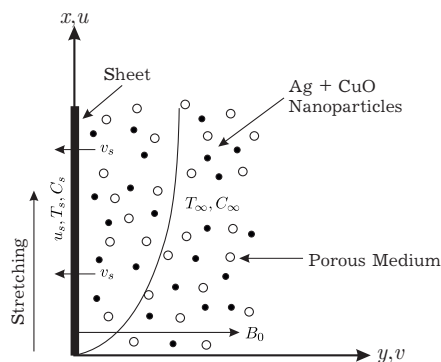
of various hybrid nanofluids over a stretching sheet. Dinarvand et al. [7] investigated the usage of hybrid nanofluid in the biomedical field by simulating a drug delivery system using CuO-Cu/blood hybrid nanofluid flow over a porous stretching sheet in the presence of a magnetic field. It was found that the magnetic field reduces the blood velocity, and blade-shaped nanoparticles provide the best heat transfer performance in the flow. Meanwhile, Aly and Pop [8] reported that the Cu-Al$_2$O$_3$/H$_2$O hybrid nanofluid works as a good heater on increasing magnetic field but turns as a better cooler on increasing Eckert number, stretching, and slip parameters. Jusoh et al. [9] found that the presence of convective boundary condition in the flow of hybrid nanofluid enhances the heat transfer rate, and the usage of kerosene as the base fluid is better than water and methanol. Wahid et al. [10] exposed that velocity slip reduces the velocity profile of Cu-Al$_2$O$_3$/H$_2$O hybrid nanofluid, but the existence of thermal radiation boosts the temperature profile of the fluid. The three-dimensional rotating flow of Ag-Al$_2$O$_3$/H$_2$O hybrid nanofluid past a stretching sheet was discussed by Shoaib et al. [11]. Whereas the unsteady flow of hybrid nanofluid over a stretching sheet was analyzed by Sreedevi et al. [12] and Santhi et al. [13]. In addition, there are also other recent studies related to hybrid nanofluid flow over a stretching sheet (see [14–22]).

Stratification and slips can occur in the flow of a heterogeneous fluid. The layering of the fluid system due to the temperature, concentration, or density differences is called stratification. For example, stratification of heterogeneous mixtures in industrial, food, and manufacturing processes [23]. Meanwhile, the inclusion of slip boundary condition in the flow of foams, suspensions, emulsions, and polymer solutions is familiar in real-life applications (e.g., melting of polymers, in drug delivery systems, microelectronic cooling systems, and micro heat exchangers) [24–26]. Rozeli et al. [27] analyzed the effects of double stratification and slips on the MHD stagnation point flow of a viscous fluid over a stretching/shrinking sheet in a porous medium. Whereas, the effects of suction and double stratification on micropolar fluid flow over a shrinking sheet were analyzed by Khashi'ie et al. [28]. Meanwhile, Hayat et al. [24] studied the effects of these parameters on the MHD flow of nanofluid over a stretching cylinder. The current study will extend these studies to the case of hybrid nanofluid, suiting the recent interest in the field of fluid dynamics. In the present study, the magnetohydrodynamics (MHD) flow of Ag-CuO/H$_2$O hybrid nanofluid, pasts a stretching sheet embedded in a porous medium, will be discussed. The mathematical formulation of the flow problem, consisting of the governing partial differential equations and boundary conditions, will be established along with the effects of slips, stratification, Brownian motion, thermophoresis, and nanoparticle volume fraction. Then, suitable similarity variables will be employed to transform the equations and boundary conditions into nonlinear ordinary differential equations before being solved numerically in Matlab using the bvp4c solver. The results in this study are original and will provide a significant contribution to the study of hybrid nanofluid in fluid dynamics and other related fields.

2. Problem geometry with mathematical formulation

Fig. 1. Geometry of the problem and coordinate system.

The geometry of the flow problem is represented by the Cartesian coordinates of x and y-axes. The velocities along these axes are given by u and v, respectively. As illustrated in Fig. 1, the working fluid, Ag-CuO/H$_2$O hybrid nanofluid, is assumed to flow over a sheet with a stretching velocity of $u_s = ax/L$, a mass transfer velocity of $v_s < 0$ for suction, and is embedded in a porous medium with a permeability of K_p. The temperature and concentration at the sheet surface are $T_s = T_0 + bx/L$ and $C_s = C_0 + dx/L$, respectively. Whereas the temperature and concentration of the free stream hybrid nanofluid are stratified at $T_\infty = T_0 + cx/L$ and $C_\infty = C_0 + ex/L$, re-

spectively. Here, a, b, c, d, and e are constants. Meanwhile, an additional effect magnetic field with strength B_0 is imposed in the perpendicular direction of the sheet, and the induced magnetic field is neglected due to the low magnetic Reynolds number. Brownian motion and thermophoresis are considered, with a Brownian diffusion coefficient, D_B and thermophoretic diffusion coefficient, D_T.

For the mathematical formulation, the nanofluid models by Buongiorno [29] and Tiwari and Das [30] are implemented to study the effects of Brownian motion, thermophoresis, and nanoparticle volume fraction on the hybrid nanofluid flow. The governing equations for the stated steady, two-dimensional flow problem are [24, 27, 31, 32]:

$$\frac{\partial u}{\partial x} + \frac{\partial v}{\partial y} = 0, \tag{1}$$

$$u\frac{\partial u}{\partial x} + v\frac{\partial u}{\partial y} = \frac{1}{\rho_{hn}}\left[\mu_{hn}\frac{\partial^2 u}{\partial y^2} - \frac{\mu_{hn}}{K_p}u - \sigma_{hn}B_0^2 u\right], \tag{2}$$

$$u\frac{\partial T}{\partial x} + v\frac{\partial T}{\partial y} = \frac{1}{(\rho C_p)_{hn}}\left[k_{hn}\frac{\partial^2 T}{\partial y^2} + \frac{[(\rho C_p)_{hn}]^2}{(\rho C_p)_{bf}}\left(D_B\frac{\partial C}{\partial y}\frac{\partial T}{\partial y} + \left(\frac{D_T}{T_\infty}\right)\left(\frac{\partial T}{\partial y}\right)^2\right)\right], \tag{3}$$

$$u\frac{\partial C}{\partial x} + v\frac{\partial C}{\partial y} = D_B\frac{\partial^2 C}{\partial y^2} + \left(\frac{D_T}{T_\infty}\right)\frac{\partial^2 T}{\partial y^2}, \tag{4}$$

which consist of the continuity equation (1), momentum equation (2), energy equation (3) and concentration equation (4). In the governing equations, ρ, μ, σ, k and ρC_p represent the density, dynamic viscosity, electrical conductivity, thermal conductivity, and heat capacity of the fluid, respectively. Meanwhile, the suffixes of hf, bf, nf, $n1$ and $n2$ are assigned for hybrid nanofluid, base fluid, CuO nanoparticles and Ag nanoparticles, respectively. The thermophysical properties of the base fluid, nanoparticles, and hybrid nanofluid are described by Devi and Devi [5] and Hayat et al. [33].

Next, the flow problem has the following boundary conditions [31]:

$$u = \lambda u_s + S_1\nu_{hn}\frac{\partial u}{\partial y}, \quad v = v_s, \quad T = T_s + S_2\frac{\partial T}{\partial y}, \quad C = C_s + S_3\frac{\partial C}{\partial y} \quad \text{at} \quad y = 0, \tag{5}$$

$$u \to 0, \quad T \to T_\infty, \quad C \to C_\infty \quad \text{as} \quad y \to \infty, \tag{6}$$

with ν as the kinematic viscosity, S_1, S_2, and S_3 are the velocity, thermal and solutal slip factors, respectively.

Local Nusselt number, Nu_x, local Sherwood number, Sh_x, and local skin friction coefficient, C_{fx} are the physical quantities of interest that correspond to the heat transfer rates, mass transfer rates, and wall shear stress, respectively. The dimensionless forms of these quantities are

$$\mathrm{Nu}_x\mathrm{Da}_x^{\frac{1}{2}} = -\frac{k_{hn}}{k_{bf}}\theta'(0), \quad \mathrm{Sh}_x\mathrm{Da}_x^{\frac{1}{2}} = -\phi'(0), \quad C_{fx}\mathrm{Re}_x\mathrm{Da}_x^{\frac{1}{2}} = 2\frac{\mu_{hn}}{\mu_{bf}}f''(0), \tag{7}$$

where $\mathrm{Da}_x = K_p/x^2$ and $\mathrm{Re}_x = xu_s/\nu_{bf}$ are the local Darcy number and Reynolds number, respectively.

3. Method of solving

Numerical computation will be carried out in Matlab using a finite-difference code-containing solver called the bvp4c, which implements the collocation formula known as the three-stage Lobatto IIIa formula [34]. The solver has a syntax of `sol = bvp4c(odefun,bcfun,solinit,options)` that integrates a system of differential equations defined in `odefun` subject to the boundary conditions specified in `bcfun` with the initial guess of solution made in `solinit` and integration settings in `options`.

For the bvp4c solver, the differential equations have to be rewritten as first-order differential equations. First, the partial differential equations and boundary conditions (1)–(6) are transformed into a

system of ordinary differential equations by using the similarity variables introduced by Mabood and Usman [31] and Reddy and Sreedevi [35]. Then, the following non-linear ordinary differential equations and boundary conditions are obtained:

$$f''' - f' + (1 - \varphi_{n1})^{2.5}(1 - \varphi_{n2})^{2.5}\mathrm{Re}\,\mathrm{Da}\left[\left(\varphi_{n2}\frac{\rho_{n2}}{\rho_{bf}} + (1 - \varphi_{n2})\left((1 - \varphi_{n1}) + \varphi_{n1}\frac{\rho_{n1}}{\rho_{bf}}\right)\right)(ff'' - f'^2)\right.$$
$$\left. - \frac{\sigma_{hn}}{\sigma_{bf}}Mf'\right] = 0, \quad (8)$$

$$\theta'' + \left[\varphi_{n2}\frac{(\rho C_p)_{n2}}{(\rho C_p)_{bf}} + (1 - \varphi_{n2})\left((1 - \varphi_{n1}) + \varphi_{n1}\frac{(\rho C_p)_{n1}}{(\rho C_p)_{bf}}\right)\right]\frac{k_{bf}}{k_{hn}}\mathrm{Pr}\left[\mathrm{Re}\,\mathrm{Da}(f\theta' - f'\theta - \xi_1 f')\right.$$
$$\left. + Nt(\theta')^2 + Nb\phi'\theta'\right] = 0, \quad (9)$$

$$\phi'' + \frac{Nt}{Nb}\theta'' - \mathrm{Re}\,\mathrm{Da}\,\mathrm{Le}(f'\phi + \xi_2 f' - f\phi') = 0, \quad (10)$$

$$f(0) = S, \quad f'(0) = \lambda + S_1^* f''(0), \quad \theta(0) = 1 - \xi_1 + S_2^* \theta'(0), \quad \phi(0) = 1 - \xi_2 + S_3^* \phi'(0),$$
$$f'(\infty) \to 0, \quad \theta(\infty) \to 0, \quad \phi(\infty) \to 0. \quad (11)$$

In the equations, f, θ, and ϕ are functions related to velocity, temperature and nanoparticle concentration profiles, respectively, with $'$ indicates differentiation with respect to η. Meanwhile, the dimensionless parameter φ is the volume fractions of individual nanoparticles, $\mathrm{Re} = (aL)/\nu_{bf}$ is the Reynolds number, $\mathrm{Da} = K_p/L^2$ is the Darcy number, $M = (\sigma_{bf}B_0^2 L)/(a\rho_{bf})$ is the magnetic field parameter, $\mathrm{Pr} = [\mu_{bf}(\rho C_p)_{bf}]/(\rho_{bf}k_{bf})$ is the Prandtl number, $\mathrm{Nb} = \left[\left(\frac{(\rho C_p)_{hn}}{(\rho C_p)_{bf}}\right)D_B(C_s - C_\infty)\right]/\nu_{bf}$ is the Brownian motion parameter, $\mathrm{Nt} = \left[\left(\frac{(\rho C_p)_{hn}}{(\rho C_p)_{bf}}\right)D_T(T_s - T_\infty)\right]/(\nu_{bf}T_\infty)$ is the thermophoresis parameter, $\mathrm{Le} = \nu_{bf}/D_B$ is the Lewis number, $\xi_1 = c/b$ is the thermal stratification parameter, $\xi_2 = e/d$ is the solutal stratification parameter, $S = -(v_s L)/(a\sqrt{K_p})$ is the suction parameter $(S > 0)$, λ is the stretching parameter, $S_1^* = (S_1\nu_{bf})/\sqrt{K_p}$ is the hydrodynamic slip parameter, $S_2^* = S_2/\sqrt{K_p}$ is the thermal slip parameter, and $S_3^* = S_3/\sqrt{K_p}$ is the solutal slip parameter.

Next, the following substitutions are introduced and substituted into (8)–(11):

$$f = y(1), \quad f' = y(1)' = y(2), \quad f'' = y(2)' = y(3), \quad f''' = y(3)',$$
$$\theta = y(4), \quad \theta' = y(4)' = y(5), \quad \theta'' = y(5)',$$
$$\phi = y(6), \quad \phi' = y(6)' = y(7), \quad \phi'' = y(7)'.$$

The resulting first-order ordinary differential equations and boundary conditions are then coded into the `odefun` and `bcfun` of the bvp4c solver, respectively. A detailed explanation and examples are shown in the study by Yahaya et al. [36]. The numerical results are recorded, analyzed, and discussed.
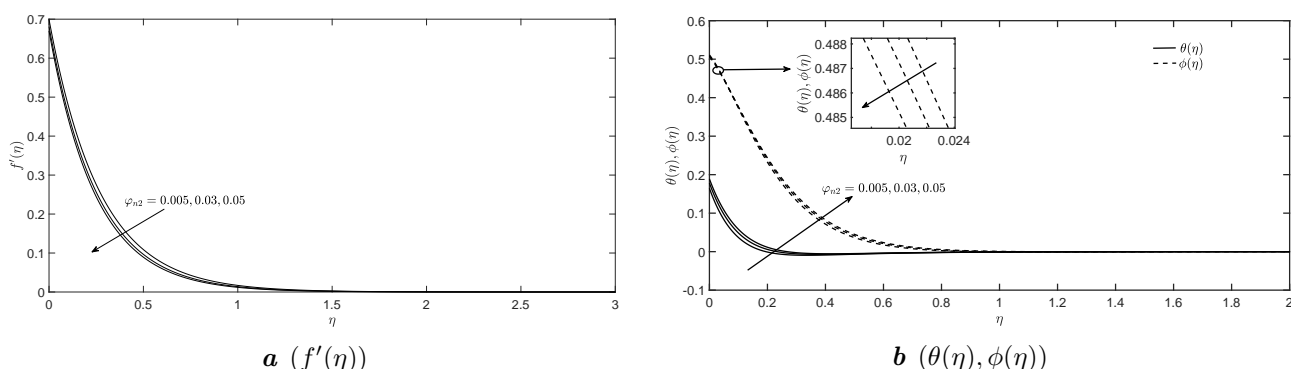
4. Results and discussion

The plots of velocity $(f'(\eta))$, temperature $(\theta(\eta))$, and concentration $(\phi(\eta))$ against η with various pertinent parameters are presented in this section. According to Pantokratoras [37], the gradients for velocity, temperature and concentration profiles at some distance away from the sheet should be zero after achieving the free stream condition (as $\eta \to \infty$) of the boundary layer flow. In this study, all profiles reach the free stream condition, stated in (11), correctly (asymptotically), which verifies the correctness of the profiles and numerical results. Besides that, the numerical results computed using the bvp4c solver are in a good agreement with the previous results by Mabood and Usman [31] that are computed using the homotopy analysis method (HAM), as shown in Table 1. However, the

temperature profiles obtained in this study show an undershoot of temperature or negative temperature. The observed behavior may be due to the high magnitude of the thermal stratification parameter used in this study. The same behavior was also reported by Srinivasacharya and Surender [38], Sarojamma et al. [39], and Khashi'ie et al. [40].

The effects of nanoparticle volume fraction of Ag, φ_{n2} on velocity profile are depicted in Fig. 2a. The increase in φ_{n2} is found to reduce the velocity profile of the hybrid nanofluid. The momentum boundary layer thickness reduces, and the skin

Table 1. Comparison of $-f''(0)$ at $\text{Pr} = 6.8$, $\text{Re} = 5$, $\lambda = 1$, $\text{Le} = 5$, $\text{Da} = M = S = \varphi_{n1} = \varphi_{n2} = \xi_1 = \xi_2 = 0$, and $\text{Nb} = \text{Nt} = 0.1$.

S_1^*	S_2^*	S_3^*	$-f''(0)$	
			Present study	Mabood and Usman [31]
1	0	0	0.50000	0.50000
0.4	0.5		0.71429	0.71429
0.5		1	0.66667	0.66667

friction coefficient decreases with the addition of φ_{n2}. Meanwhile, the temperature profile in Fig. 2b shows an improvement with the increasing value of φ_{n2}. Khashi'ie et al. [41] stated that nanoparticles dissipate heat energy. Thus, adding more nanoparticles will raise the temperature of the hybrid nanofluid and causes the temperature profile to increase. Since Ag nanoparticles have high thermal conductivity, the introduction of more of these nanoparticles into the hybrid nanofluid enhances the Nusselt number $\left[= -\frac{k_{hn}}{k_{bf}}\theta'(0)\right]$, as shown in Table 2. Thus, incorporating a certain amount of metallic nanoparticle Ag into the hybrid nanofluid can improve the heat transfer performance of the fluid. However, as shown in Fig. 2b, the increase in φ_{n2} lowers the concentration profile of the hybrid nanofluid near the sheet. After some distance from the sheet, the concentration profile improves with φ_{n2}.
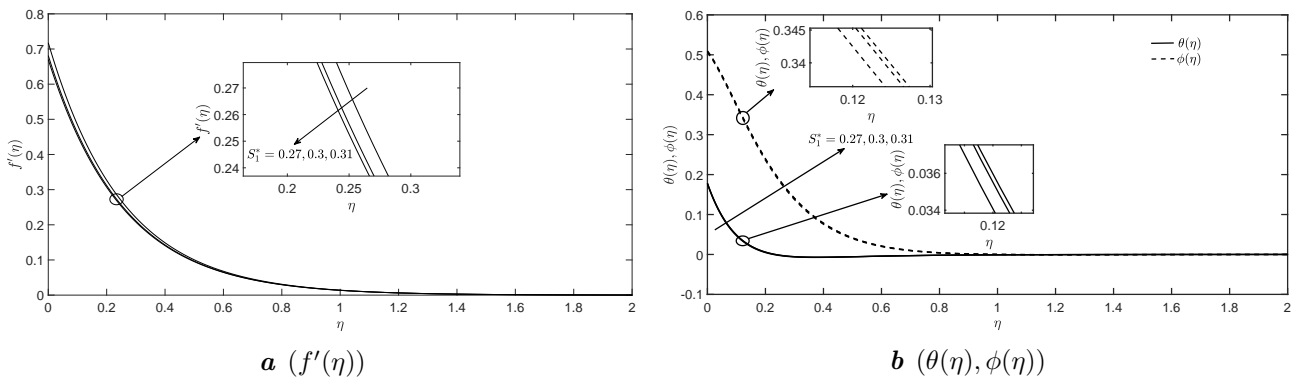

a $(f'(\eta))$ b $(\theta(\eta), \phi(\eta))$

Fig. 2. Velocity, temperature and concentration profiles with varying values of nanoparticle volume fraction of Ag, φ_{n2}.
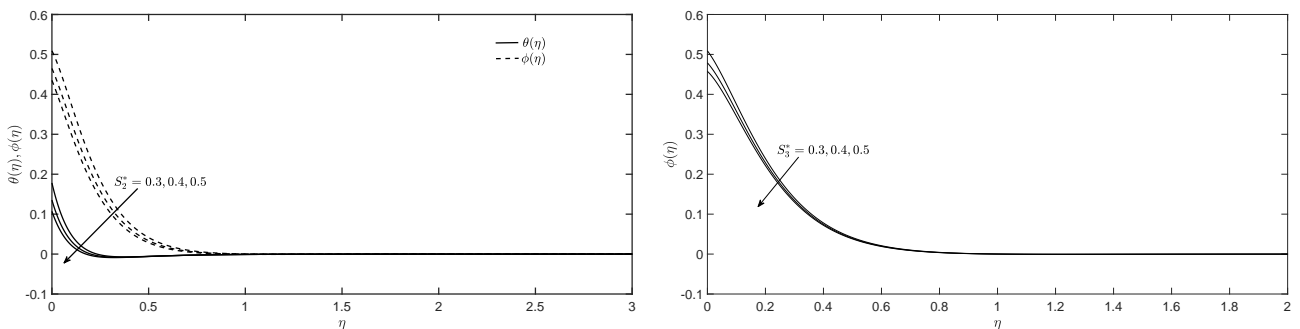
Next, Fig. 3a illustrates the effects of the hydrodynamic slip parameter, S_1^* on the velocity profile. It is observed that the increase in S_1^* diminishes the velocity profile of the hybrid nanofluid. Physically, hydrodynamic slip causes the fluid velocity near the sheet to be unequal to the stretching sheet. The higher the value of S_1^*, the lower the velocity of the stretching sheet transferred to the hybrid nanofluid. Besides that, the increase in S_1^* produces friction force that enables more fluid to slip past the stretching sheet, which lowers the hybrid nanofluid velocity and raises the temperature. As shown in Fig. 3b, the temperature and concentration profiles increase with S_1^*. The thickness of thermal and concentration boundary layers elevates and reduces the values of $-\theta'(0)$ and $-\phi'(0)$. The Nusselt number and Sherwood number decrease with the rise of S_1^*, as tabulated in Table 2. Contrary, the augmentation of the thermal slip parameter, S_2^* reduces the temperature and concentration profiles displayed in Fig. 4. The decreasing value of the Nusselt number obtained in Table 2 indicates that the rise in S_2^* inhibits the heat transfer performance of the fluid. Less heat is transferred from the hot stretching sheet to the surrounding hybrid nanofluid, which causes the reduction of fluid temperature. Similarly, the increase in solutal slip parameter, S_3^* reduces the concentration profile in Fig. 5 and lowers the mass transfer performance of the hybrid nanofluid, as obtained in Table 2.

Table 2. Values of $C_{fx}\mathrm{Re}_x\mathrm{Da}_x^{\frac{1}{2}}$, $\mathrm{Nu}_x\mathrm{Da}_x^{\frac{1}{2}}$ and $\mathrm{Sh}_x\mathrm{Da}_x^{\frac{1}{2}}$ when $\varphi_{n1}=0.1$, $\mathrm{Da}=0.5$, $\mathrm{Le}=2$, $\mathrm{Pr}=6.2$, $\lambda=1.48$, $M=0.1$ and $\mathrm{Re}=5$.

φ_{n2}	S	S_1^*	S_2^*	S_3^*	ξ_1	ξ_2	Nt	Nb	$C_{fx}\mathrm{Re}_x\mathrm{Da}_x^{\frac{1}{2}}$	$\mathrm{Nu}_x\mathrm{Da}_x^{\frac{1}{2}}$	$\mathrm{Sh}_x\mathrm{Da}_x^{\frac{1}{2}}$
0.005	0.95	0.3	0.3	0.3	0.2	0.2	0.1	0.1	−6.85857	2.84746	0.96323
0.03		0.27							−7.92900	3.00621	0.97851
		0.3	0.4						−7.47832	2.40401	1.11739
			0.5						−7.47832	2.00515	1.21638
			0.3	0.4					−7.47832	3.00162	0.80274
				0.5					−7.47832	3.00374	0.68472
				0.3	0.1				−7.47832	3.29969	0.89670
					0.2	0.1			−7.47832	2.99507	1.14797
						0.2			−7.47832	2.99861	0.96991
						0.3			−7.47832	2.69641	1.04343
						0.2	0.3		−7.47832	3.00213	0.79185
							0.2	0.13	−7.47832	2.98892	0.74926
								0.15	−7.47832	2.98240	0.60312
							0.1	0.2	−7.47832	2.96746	1.34824
								0.3	−7.47832	2.93504	1.47447
		0.31						0.1	−7.33966	2.99622	0.96721
	0.96	0.3							−7.50009	3.00354	0.97570
	0.94								−7.45648	2.99364	0.96411
0.05	0.95								−7.99000	3.12168	0.97705

a $(f'(\eta))$ *b* $(\theta(\eta),\phi(\eta))$

Fig. 3. Velocity, temperature and concentration profiles with varying values of hydrodynamic slip parameter, S_1^*.
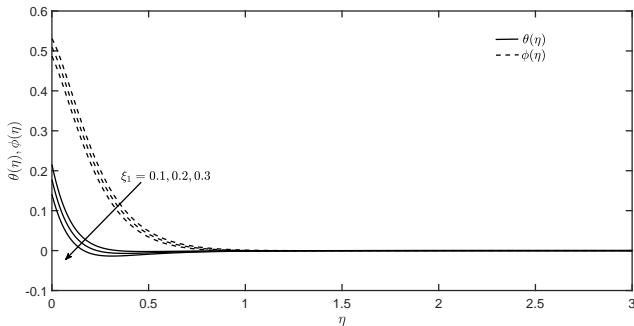

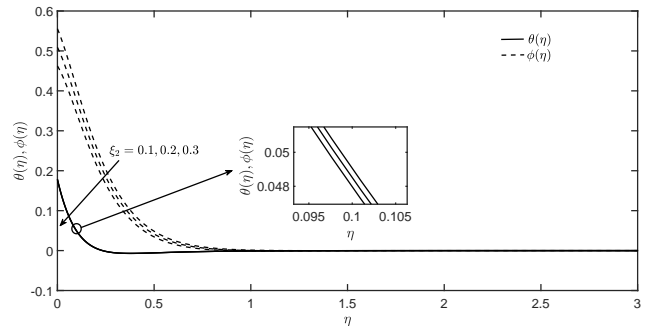**Fig. 4.** Temperature and concentration profiles with varying values of thermal slip parameter, S_2^*.

Fig. 5. Concentration profile with varying values of solutal slip parameter, S_3^*.

In Fig. 6, the temperature and concentration profiles are observed to decrease as ξ_1 increases. Similar behavior is observed in Fig. 7 for the increasing value of ξ_2. However, the enhancement of ξ_1 and ξ_2 affects the Nusselt number and Sherwood number differently, as seen in Table 2. The increase in thermal stratification parameter $[\xi_1 = c/b]$ signifies the augmentation of ambient temperature or re-

duction of the surface temperature. Hence, the difference between ambient and surface temperatures diminishes as ξ_1 increases. As a result, the temperature gradient decreases, reducing the heat transfer rate and temperature profile of the hybrid nanofluid. The reduced concentration boundary layer thickness raises the concentration gradient and enhances the Sherwood number. Meanwhile, the Sherwood number drops when ξ_2 increases. The rise in solutal stratification parameter $[\xi_2 = e/d]$ describes the enhancement of ambient fluid concentration or depletion in surface concentration. Thus, augmentation of ξ_2 promotes the reduction of the concentration gradient that reduces the Sherwood number.
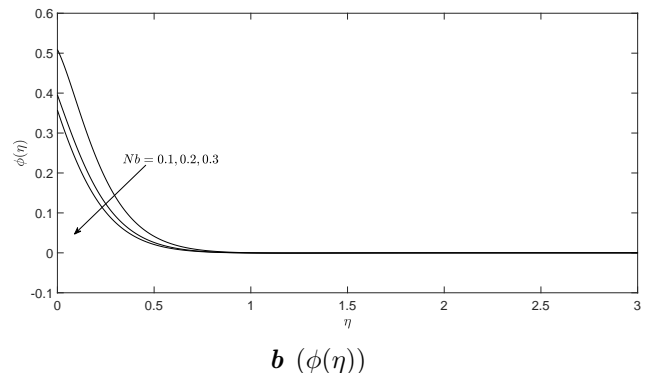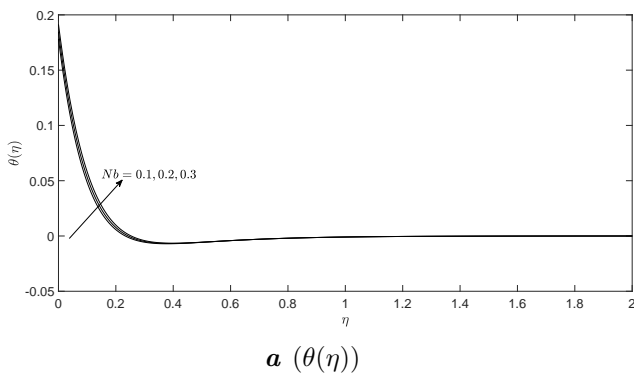

Fig. 6. Temperature and concentration profiles with varying values of thermal stratification parameter, ξ_1.

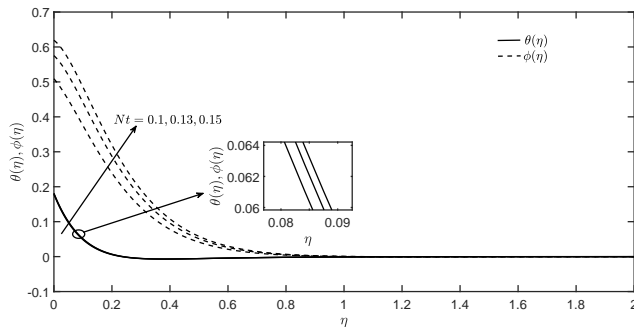**Fig. 7.** Temperature and concentration profiles with varying values of solutal stratification parameter, ξ_2.

Meanwhile, the Brownian motion in the hybrid nanofluid flow enhances the fluid temperature but reduces the concentration, as observed in Figs. 8a and 8b, respectively. The random movement of nanoparticles in the base fluid stimulates collisions between them, which generate kinetic energy that can be converted into heat energy. Hence, the increase in Nb raises the temperature profile of the hybrid nanofluid and reduces the Nusselt number, as obtained in Table 2. However, the increment of Nb helps in improving the mass transfer performance of the hybrid nanofluid, as depicted by the increase in Sherwood number in Table 2.
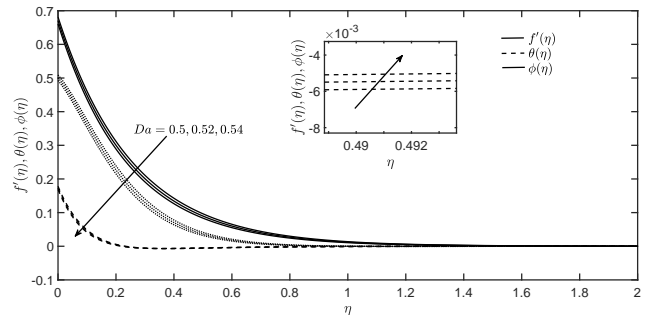

a $(\theta(\eta))$

b $(\phi(\eta))$

Fig. 8. Temperature and concentration profiles with varying values of Brownian motion parameter, Nb.

The incorporation of thermophoresis in the hybrid nanofluid flow increases the temperature and concentration profiles of the hybrid nanofluid, as presented in Fig. 9. The movement of hot nanoparticles near the hot sheet to the surrounding cold hybrid nanofluid enhances the temperature and concentration of the fluid. Thus, reducing the temperature and concentration gradients then lowers the rates of heat and mass transfers, as shown in Table 2.

The effects of Darcy number, Da on the velocity, temperature and concentration profiles are displayed in Fig. 10. Darcy number is a parameter related to the permeability of the porous medium. The increase in Da causes the reduction of the velocity, temperature and concentration profiles of the hybrid nanofluid. However, it is observed in Fig. 10 that the temperature profile increases after some distance away from the sheet. The momentum, thermal and concentration boundary layers become thinner as Da increases.

Fig. 9. Temperature and concentration profiles with varying values of thermophoresis parameter, Nt.

Fig. 10. Velocity, temperature and concentration profiles with varying values of Darcy number, Da.

5. Conclusion

The MHD flow of Ag-CuO/H$_2$O hybrid nanofluid over a permeable stretching sheet embedded in a porous medium with other effects of slips and stratification are analyzed and discussed. The Buongiorno and the Tiwari and Das nanofluid models are incorporated into the governing partial differential equations and boundary conditions. Then, these equations are simplified into a system of ordinary differential equations using appropriate similarity variables and solved numerically using the bvp4c solver. The increase in hydrodynamic slip parameter reduces the velocity profile of the hybrid nanofluid. Meanwhile, the temperature and concentration profiles diminished with the rise in thermal slip and stratification parameters. Besides that, the concentration profile is reduced by the augmentation of solutal slip and stratification parameters.

[1] Shanmugapriya M., Sundareswaran R., Senthil Kumar P. Heat and mass transfer enhancement of MHD hybrid nanofluid flow in the presence of activation energy. International Journal of Chemical Engineering. **2021**, 9473226 (2021).

[2] Hayat T., Nadeem S. Heat transfer enhancement with Ag-CuO/water hybrid nanofluid. Results in Physics. **7**, 2317–2324 (2017).

[3] McCash L. B., Zehra I., Al-Zubaidi A., Amjad M., Abbas N., Nadeem S. Combined effects of binary chemical reaction/activation energy on the flow of Sisko fluid over a curved surface. Crystals. **11** (8), 967 (2021).

[4] Gangadhar K., Edukondala Nayak R., Venkata Subba Rao M. Buoyancy effect on mixed convection boundary layer flow of Casson fluid over a non linear stretched sheet using the spectral relaxation method. International Journal of Ambient Energy. **43** (1), 1994–2002 (2022).

[5] Devi S. A., Devi S. S. U. Numerical investigation of hydromagnetic hybrid Cu-Al$_2$O$_3$/water nanofluid flow over a permeable stretching sheet with suction. International Journal of Nonlinear Sciences and Numerical Simulation. **17** (5), 249–257 (2016).

[6] Prakash M., Devi S. Hydromagnetic hybrid Al$_2$O$_3$-Cu/water nanofluid flow over a slendering stretching sheet with prescribed surface temperature. Asian Journal of Research in Social Sciences and Humanities. **6** (9), 1921–1936 (2016).

[7] Dinarvand S., Rostami M. N., Dinarvand R., Pop I. Improvement of drug delivery micro-circulatory system with a novel pattern of CuO-Cu/blood hybrid nanofluid flow towards a porous stretching sheet. International Journal of Numerical Methods for Heat & Fluid Flow. **29** (11), 4408–4429 (2019).

[8] Aly E. H., Pop I. MHD flow and heat transfer near stagnation point over a stretching/shrinking surface with partial slip and viscous dissipation: Hybrid nanofluid versus nanofluid. Powder Technology. **367**, 192–205 (2020).

[9] Jusoh R., Naganthran K., Jamaludin A., Ariff M. H., Basir M. F. M., Pop I. Mathematical analysis of the flow and heat transfer of Ag-Cu hybrid nanofluid over a stretching/shrinking surface with convective

boundary condition and viscous dissipation. Data Analytics and Applied Mathematics (DAAM). **1** (1), 11–22 (2020).

[10] Wahid N. S., Md Arifin N., Turkyilmazoglu M., Hafidzuddin M. E. H., Abd Rahmin N. A. MHD hybrid Cu-Al$_2$O$_3$/water nanofluid flow with thermal radiation and partial slip past a permeable stretching surface: analytical solution. Journal of Nano Research. **64**, 75–91 (2020).

[11] Shoaib M., Raja M. A. Z., Sabir M. T., Islam S., Shah Z., Kumam P., Alrabaiah H. Numerical investigation for rotating flow of MHD hybrid nanofluid with thermal radiation over a stretching sheet. Scientific Reports. **10** (1), 18533 (2020).

[12] Sreedevi P., Sudarsana Reddy P., Chamkha A. Heat and mass transfer analysis of unsteady hybrid nanofluid flow over a stretching sheet with thermal radiation. SN Applied Sciences. **2** (7), 1222 (2020).

[13] Santhi M., Suryanarayana Rao K. V., Sudarsana Reddy P., Sreedevi P. Heat and mass transfer characteristics of radiative hybrid nanofluid flow over a stretching sheet with chemical reaction. Heat Transfer. **50** (3), 2929–2949 (2021).

[14] Khashi'ie N. S., Arifin N. M., Pop I., Nazar R., Hafidzuddin E. H., Wahi N. Flow and heat transfer past a permeable power-law deformable plate with orthogonal shear in a hybrid nanofluid. Alexandria Engineering Journal. **59** (3), 1869–1879 (2020).

[15] Khashi'ie N. S., Arifin N. M., Pop I., Nazar R., Hafidzuddin E. H., Wahi N. Thermal marangoni flow past a permeable stretching/shrinking sheet in a hybrid Cu-Al$_2$O$_3$/water nanofluid. Sains Malaysiana. **49** (1), 211–222 (2020).

[16] Wahid N. S., Arifin N. M., Khashi'ie N. S., Pop I., Bachok N., Hafidzuddin M. E. H. Flow and heat transfer of hybrid nanofluid induced by an exponentially stretching/shrinking curved surface. Case Studies in Thermal Engineering. **25**, 100982 (2021).

[17] Venkateswarlu B., Satya Narayana P. V. Cu-Al$_2$A$_3$/H$_2$O hybrid nanofluid flow past a porous stretching sheet due to temperature-dependent viscosity and viscous dissipation. Heat Transfer. **50** (1), 432–449 (2021).

[18] Yahya A. U., Salamat N., Huang W. H., Siddique I., Abdal S., Hussain S. Thermal charactristics for the flow of williamson hybrid nanofluid (MoS$_2$+ZnO) based with engine oil over a streched sheet. Case Studies in Thermal Engineering. **26**, 101196 (2021).

[19] Puneeth V., Manjunatha S., Madhukesh J. K., Ramesh G. K. Three dimensional mixed convection flow of hybrid casson nanofluid past a non-linear stretching surface: A modified Buongiornonï̈S's model aspects. Chaos, Solitons & Fractals. **152**, 111428 (2021).

[20] Kumar T. S. Hybrid nanofluid slip flow and heat transfer over a stretching surface. Partial Differential Equations in Applied Mathematics. **4**, 100070 (2021).

[21] Roşca N. C., Pop I. Hybrid nanofluids flows determined by a permeable power-law stretching/shrinking sheet modulated by orthogonal surface shear. Entropy. **23** (7), 813 (2021).

[22] Kho Y. B., Jusoh R., Salleh M. Z., Mohamed M. K. A., Ismail Z., Hamid R. A. Inclusion of viscous dissipation on the boundary layer flow of Cu-TiO$_2$ hybrid nanofluid over stretching/shrinking sheet. Journal of Advanced Research in Fluid Mechanics and Thermal Sciences. **88** (2), 64–79 (2021).

[23] Ibrahim W., Makinde O. D. The effect of double stratification on boundary-layer flow and heat transfer of nanofluid over a vertical plate. Computers & Fluids. **86**, 433–441 (2013).

[24] Hayat T., Nassem A., Khan M. I., Farooq M., Al-Saedi A. Magnetohydrodynamic (MHD) flow of nanofluid with double stratification and slip conditions. Physics and Chemistry of Liquids. **56** (2), 189–208 (2018).

[25] Sarojamma G., Lakshmi R. V., Sreelakshmi K., Vajravelu K. Dual stratification effects on double-diffusive convective heat and mass transfer of a sheet-driven micropolar fluid flow. Journal of King Saud University – Science. **32** (1), 366–376 (2020).

[26] Wahid N. S., Arifin N. M., Khashi'ie N. S., Pop I. Hybrid nanofluid slip flow over an exponentially stretching/shrinking permeable sheet with heat generation. Mathematics. **9** (1), 30 (2020).

[27] Rozeli N. S., Som A. N. M., Arifin N. M., Ali F. M., Abd Ghani A. Double stratified MHD stagnation point slip flow over a permeable shrinking/stretching surface in a porous medium. Journal of Advanced Research in Fluid Mechanics and Thermal Sciences. **90** (2), 64–72 (2022).

[28] Khashi'ie N. S., Wahi N., Arifin N. M., Ghani A. A., Hamzah K. B. Effect of suction on the MHD flow in a doubly-stratified micropolar fluid over a shrinking sheet. Mathematical Modeling and Computing. **9** (1), 92–100 (2022).

[29] Buongiorno J. Convective transport in nanofluids. Journal of Heat Transfer. **128** (3), 240–250 (2005).

[30] Tiwari R. K., Das M. K. Heat transfer augmentation in a two-sided lid-driven differentially heated square cavity utilizing nanofluids. International Journal of Heat and Mass Transfer. **50** (9–10), 2002–2018 (2007).

[31] Mabood F., Usman H. Multiple slips effects on MHD thermo-solutal flow in porous media saturated by nanofluid. Mathematical Modelling of Engineering Problems. **6** (4), 502–510 (2019).

[32] Ijaz M., Ayub M. Activation energy and dual stratification effects for Walter-B fluid flow in view of Cattaneo–Christov double diffusion. Heliyon. **5** (6), E01815 (2019).

[33] Hayat T., Nawaz S., Alsaedi A., Rafiq M. Mixed convective peristaltic flow of water based nanofluids with Joule heating and convective boundary conditions. PLoS One. **11** (4), 0153537 (2016).

[34] Keskin A. Ü. Solution of BVPs using bvp4c and bvp5c of MATLAB. In: Boundary Value Problems for Engineers. Springer, Cham (2019).

[35] Sudarsana Reddy P., Sreedevi P. Impact of chemical reaction and double stratification on heat and mass transfer characteristics of nanofluid flow over porous stretching sheet with thermal radiation. International Journal of Ambient Energy. **43** (1), 1626–1636 (2022).

[36] Yahaya R. I., Arifin N. M., Nazar R. M., Pop I. Oblique stagnation-point flow past a shrinking surface in a Cu-Al$_2$O$_3$/H$_2$O hybrid nanofluid. Sains Malaysiana. **50** (10), 3139–3152 (2021).

[37] Pantokratoras A. A common error made in investigation of boundary layer flows. Applied Mathematical Modelling. **33** (1), 413–422 (2009).

[38] Srinivasacharya D., Surender O. Effect of double stratification on mixed convection boundary layer flow of a nanofluid past a vertical plate in a porous medium. Applied Nanoscience. **5** (1), 29–38 (2015).

[39] Sarojamma G., Lakshmi R. V., Sreelakshmi K., Vajravelu K. Dual stratification effects on double-diffusive convective heat and mass transfer of a sheet-driven micropolar fluid flow. Journal of King Saud University – Science. **32** (1), 366–376 (2020).

[40] Khashi'ie N. S., Arifin N. M., Rashidi M. M., Hafidzuddin E. H., Wahi N. Magnetohydrodynamics (MHD) stagnation point flow past a shrinking/stretching surface with double stratification effect in a porous medium. Journal of Thermal Analysis and Calorimetry. **139** (6), 3635–3648 (2020).

[41] Khashi'ie N. S., Hafidzuddin E. H., Arifin N. M., Wahi N. Stagnation point flow of hybrid nanofluid over a permeable vertical stretching/shrinking cylinder with thermal stratification effect. CFD Letters. **12** (2), 80–94 (2020).

Магнітногідродинамічний потік гібридного нанофлюїду на листі, що розтягується: ефект подвійної стратифікації та багаторазового ковзання

Яхая Р. І.[1], Алі Ф. М.[1,2], Аріфін Н. М.[1,2], Хашіє Н. С.[3], Іса С. С. П. М.[1,4]

[1]*Інститут математичних досліджень,*
Університет Путра Малайзії,
43400 Серданг, Селангор, Малайзія
[2]*Факультет математики,*
Університет Путра Малайзія,
43400 Серданг, Селангор, Малайзія
[3]*Факультет технології машинобудування та виробництва,*
Технічний університет Малайзії в Мелаці,
Ханг Туа Джая, 76100 Дуріан Тунггал, Малакка, Малайзія
[4]*Центр фундаментальних досліджень для сільськогосподарських наук,*
Університет Путра Малайзії,
43400 Серданг, Селангор, Малайзія

Дослідження гібридних нанофлюїдів, що протікають через різні фізичні геометрії та за різних умов, є популярними серед дослідників, які хочуть зрозуміти поведінку цих рідин. У цьому дослідженні аналізуються чисельні розв'язки для потоку гібридної нанорідини Ag-CuO/H_2O по листі, який розтягується, із ефектом всмоктування, магнітним полем, подвійною стратифікацією та багаторазовим ковзанням. Для опису задачі потоку вводяться основні рівняння та крайові умови. Потім застосовуються змінні подібності з метою перетворення рівнянь у нелінійні звичайні диференціальні рівняння та крайові умови. Чисельне обчислення задачі виконано в Matlab (вирішувач bvp4c), а результати подані в таблицях і графіках. Встановлено, що збільшення параметрів ковзання та стратифікації розчинів зменшує число Шервуда. Водночас збільшення параметрів теплового ковзання та стратифікації знижує число Нуссельта. Зі збільшенням параметра гідродинамічного ковзання спостерігається збільшення коефіцієнта поверхневого тертя.

Ключові слова: *гібридний нанофлюїд, подвійна стратифікація, ковзання, МГД, лист, що розтягується.*